



## **Review on two-phase flow boiling in oblique fined microchannel heat sink with different channel cross section**

**R.Vinoth\*, Naveen Kumar Nagalli, M Parthiban**

**Department of Mechanical Engineering, Adhiyamaan College of Engineering, Hosur, Tamil Nadu 635109, India.**

**Abstract :** The research era and development on two-phase flow boiling will give a tremendous choice in various application fields. In spite of this progression, there arise disarray forms under the different streams of the cross-section, oblique fins and types of fluid being used. This study deals on various cross-sections such as rectangular, square, triangle and with variable aspect ratio of the microchannel. The paper focuses on the behavior of different types of fluid used in a microchannel with various thermo-physical properties. The formulated growth in the fields of flow boiling from the introductory to the modern changes is enumerated in both the ways of experimental as well as numerical. In addition to that, this paper concerns the bubble growth rate and heat transfer characteristics of flow boiling experiments. Numerical solutions and their correlations with their experimental data are also summarised. The stimulated improvements in various aspects of microchannel era in experimental and theoretical data are tabulated. Based on the consolidated database a new model approach on two-phase flow boiling has resulted out.

**Keywords :** Microchannel, Flow boiling, Oblique fins, Heat transfer rate.

### **1.Introduction**

In the recent years the research in the field of two-phase flow heat transfer at a microscale level has been persistently increasing due to the quickie growth of the technological applications that involve the transfer of high heat rate in a relatively small space and volume. All technical field solutions are in demand that retards as little as possible without compromising on performance. There are particular issues such as an increase in energy seek, space limitations and material savings have emphasized the necessity for miniaturized light-weight heat exchangers. However, it is strictly difficult, or even impossible, to come across the thermal management requirement with either conservative air cooling or liquid cooling without applying any chillness. Thermal managing of high heat-flux electronic devices had charmed significant consideration in current years. The heat is ejected by a coolant and rejected to the atmosphere. As heat flux heights are kept on increasing, the capability should be increased to sustain tolerable device temperatures for static ambient air temperature. It is not that the thermal resistance had only the coolant's convection resistance, but also the conduction resistance across the device. Refrigeration cooling is an active mean of prominently reducing the coolant's temperature by maintaining the acceptable device temperatures when dispersing very high heat fluxes. In desktop computers,

**International Journal of ChemTech Research, 2018,11(05): 220-235.**

**DOI= <http://dx.doi.org/10.20902/IJCTR.2018.110525>**

heat sinks are used to keep the temperature cool in CPU and graphics processors. Heat sinks comprise of high-power semiconductor devices such as lasers, power transistors and LED (Light Emitting Diodes). The Air has taken the medium of cooling to make the surface area of contact with the microchannel heat sink. Material selection, the velocity of the air, design parameters and surface treatment are some of the sensible factors in which the heat transfer performance get affected. Attachment methods for heat sink and thermal boundary materials also affect the subsequent temperature of the integrated circuit. To enhance the heat transfer performance, the air gap between the heat sink and device is filled by thermal adhesives. The work by Tuckerman and Pease in the early 1980s created attentiveness in the use of microchannel heat sinks as a means for driving away the considerable amount of heat from high heat-flux devices.

They found applications in electronic devices and aerospace systems. Research in conventional type focuses on single phase flow, but the revolutionary trend focuses on two-phase flow boiling in microchannel heat exchanger. Heat sinks are categorized into single phase or two-phase based on their boiling of liquid inside the channel. Coolant flow rate and channel wall are the two parameters that determine the type of phase operating regime. For single phase flow, the heat flux is maintained at a fixed rate so that the coolant may retain in the liquid state. When the flow rate is decreased, the coolant inside the channel reaches its boiling point and thus flow boiling takes place which resulted out two-phase heat sink.

### 1.1 Oblique microchannel heat sink

The continuous fins are sectioned at a particular angle, which leads to the oblique finned microchannel. The oblique finned microchannel has supplementary improvements over the later without any considerable increase in size. There is a secondary flow in addition to the primary flow that resulted out the increase in the overall heat transfer and a decrease in thermal and hydrodynamic boundary layers. A heat sink transfers heat energy from a higher temperature to a lower temperature through a fluid medium. The fluid medium is usually the air, but in some instances, it can be of water, refrigerants or oil. If the fluid medium is taken as water, the 'heat sink' is subsequently called a cold plate.

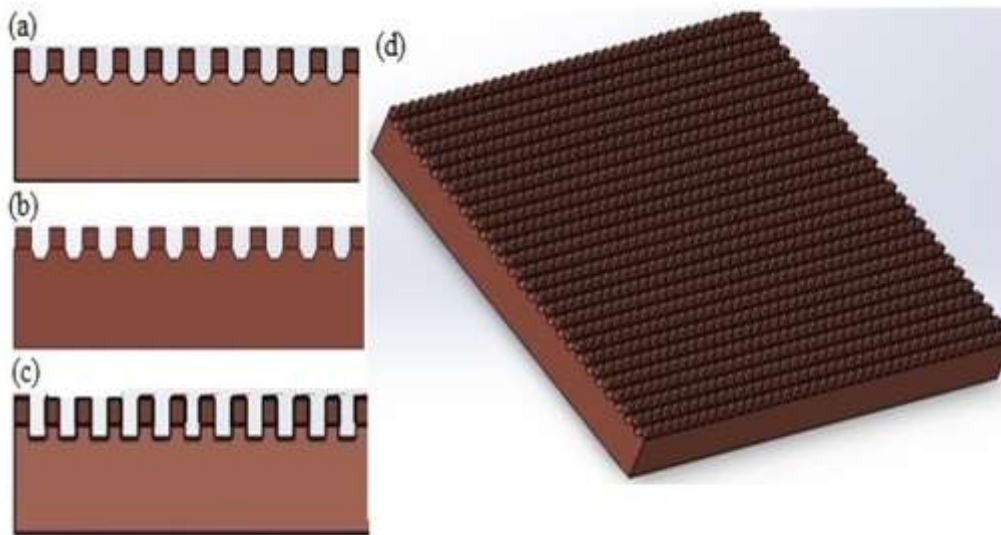


**Figure 1 Different channel cross-sections**

The figure 1 shows that three different types of channel cross section such as (a) semicircular, (b) Trapezoidal, (c) Square and (d) oblique finned microchannel heat sink. The splintering of continuous fins into oblique fins leads to re-initialization of the hydrodynamic and thermal boundary layer at the primary edge of each oblique fin, which in turn reduces the thickness of boundary layer. The redevelopment of inlet effect makes the flow be always in the emerging state thus resulting in improved heat transfer. Due to the occurrence of smaller oblique channels, diversion of a small fraction of fluid flow into the adjacent main channels will occur. This fluid mixing creates the secondary flow which increases the heat transfer performance.

## 1.2 Two-phase flow boiling

For several decades, flow boiling in small diameter channels has been recognized as an effective means of dissipating heat at very high rates. To remove the heat from planar surfaces, flow boiling can be achieved inside multiple parallel channels that are formed in a high conductivity substrate, a “microchannel heat sink.” Single-phase microchannel heat sinks have been explored quite extensively, especially in conjunction with electronics cooling. These devices are very compact and lightweight and their thermal merits are readily recognized for laminar flow. The figure 2 shows that flow boiling in microchannel heat sink with various flow patterns.

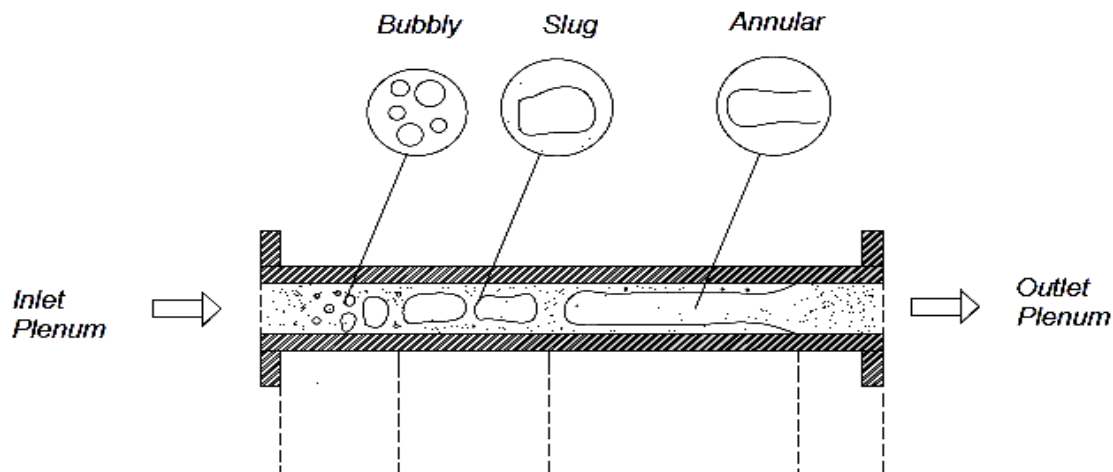


**Figure 2 Flow boiling in microchannel with flow patterns**

The heat transfer coefficient is inversely proportional to hydraulic diameter and very high heat transfer coefficient can be achieved just by using very small diameters. However, single-phase microchannel heat sinks intended for high flux situations that produce high-pressure drop since they rely on sensible heat increase to achieve the cooling, a large temperature gradient in the direction of fluid flow. Two-phase microchannel heat sinks offer several advantages over their single-phase counterparts. First, they can achieve far greater heat transfer coefficient by utilizing the coolant’s latent heat. This means a far smaller coolant flow rate is essential to dissipate the same amount of heat as that of a single-phase heat sink, which helps to reduce coolant inventory for the entire cooling system. Additionally, by relying on mostly latent heat transfer, two-phase heat sinks provide better axial temperature uniformity, maintaining Temperatures close to the coolant’s saturation temperature.

## 2. Experimental and numerical studies on microchannel heat sink

### 2.1 Experimental studies on microchannel cross section

It is evident that, heat transfer enhancement in microchannels not only dependent on the fluid used and type of boiling takes place inside the channel. The cross-section is one of the major parameters which plays a vital role in heat transfer. **Jingru Zhang et al. [1]** apparently examined the same input parameters for two different cross-sections where there was a rapid change in performance. Hence increasing or decreasing the surface area will lead to reduced pressure drop and greater heat transfer performance. **Melanie Derby et al. [2]** had conducted experimental investigations on condensation heat transfer. They used R134a as a fluid in the square, triangular and semi-circular multiple parallel mini-channels which was cooled on three sides. They also studied the comparison of square, triangular, and semi-circular channel geometries with the similar hydraulic diameter of 1 mm. Numerical studies by Wang and Rose found that significant heat transfer enhancement through surface tension was at the millimeter scale. Through the experiment, they observed that the Lack of surface tension effects was perhaps in part influenced by three-sided cooling boundary conditions. Moreover, they concluded the Shah correlation as best-predicted data with an average MAE between 20% and

30% for all test section geometries. **Tu-chieh Hung et al. [3]** had performed a numerical analysis to examine the heat transfer characteristics of a double-layered Microchannel Heat sink. They analysed that the heat transfer performance of the heat sink was improved for the system with substrate materials having a superior thermal conductivity ratio. Through the numerical study, they observed pressure drop reduced with the channel aspect ratio and channel Width ratio. Finally, from the results they concluded that the thermal performance of the double-layered microchannel heat sink is better than that of the single-layered one by an average of 6.3%.

**Sylwia Szczukiewicz et al. [4]** experimentally investigated the two-phase Flow-boiling of R245fa, R236fa and R1234ze (E) in  $100 \times 100 \mu\text{m}^2$  parallel silicon multi microchannels. They were considered as with and without the inlet micro-orifices for cooling future of 3D-ICs. They observed the significant flow instabilities, backflow, and non-uniform flow distribution among the channels in the micro-evaporator without any inlet restrictions (micro-orifices). Through the experimental tests, it was concluded that the maximum junction temperature of the micro-evaporator  $T_{\text{IR}}$  was  $57^\circ\text{C}$  for R245fa,  $50.3^\circ\text{C}$  for R236fa, and  $43.1^\circ\text{C}$  for R1234ze (E). It was lower than the given temperature having limit of  $85^\circ\text{C}$ . In addition to the flow analysis of Sylwia Szczukiewicz et al. [4] **Ahmad Odaymet et al. [5]** conducted an experimental research on slug flow for condensation in a single square microchannel. Deionized water is used as the fluid in a controlled steam generator. Six different types of flow regimes were observed. They obtained the experimental results from flow visualization images which showed that bubble velocity significantly influenced by departure of each new bubble followed by new liquid slug from the microchannel entrance. They observed that the coalescence between neighbouring bubbles leads to increase in bubbles velocity. They also compared the obtained experimental data with condensation heat transfer correlations from the literature. In contrary to that, they found that the correlation of Dobson and Chato gives good predictions having an overall heat transfer with maximum deviation of 10% at higher mass fluxes.

**Aymen Megahed et al. [6]** experimentally investigated the characteristics of flow boiling in a cross-linked microchannel heat sink. The rapid bubble formation, growth and delayed bubble detachment from the nucleation sites had been observed. Through the experiment authors found that the two-phase pressure drop increased with exit quality at  $x_{e,0} < 0.3$ . Heat transfer coefficient was high when compared with straight linked microchannels, two-phase Frictional pressure drop rose by a factor of 1.6-2.0. **Yuan Wang et al. [7]** conducted an experiment on flow boiling heat transfer in several aspect ratio. The FC-72 is used as working fluid under different channels with hydraulic diameters (571, 762, and  $1454 \mu\text{m}$ ) and aspect ratios of (20, 20 and 10) respectively. Based on speed visualization results and channel surface temperature profiles, they found that Onset of nucleate boiling (ONB) is higher at higher mass flux, Critical heat flux (CHF) increases with increasing hydraulic diameter. Also, this shows that the local heat transfer coefficient increase with a decrease in hydraulic diameter. Through the obtained results, they concluded that Convective Boiling is more dominant heat transfer mechanism. Unique channel geometry is also the reasons for flow regions and heat transfer mechanisms. **Tannaz Harirchian et al. [8]** conducted an experiment on effects channel dimension, heat flux and mass flux in the flow boiling regimes in microchannels. The perforated dielectric fluid (fluorinert FC-77) is used with a mass flux ( $225$ -  $1420 \text{ kg/m}^2\text{s}$ ).

The five flow regimes such as bubbly, churn, wispy-annular, slug and annular flows were observed. The visualization results and heat transfer data shows that flow regimes in microchannel of width  $400 \mu\text{m}$  and larger are of similar with nucleate boiling. Being more dominant in these channels with a broad range of heat flux whereas flow regimes in smaller microchannel have different bubble nucleation are suppressed in walls at relatively low heat flux.

## 2.2 Numerical studies on the microchannel cross section

Since the number of articles are being published in the heat removal section, there is always a gap lying between the numerical studies and two-phase flow as **Talimi V et al. [9]** said in 2011. In order to overcome this many numerical simulations are carried out in two-phase flow, some of the investigations are discussed here. **John P. McHale et al. [10]** numerically investigated the heat transfer performance in the thermal entrance region of trapezoidal microchannels without any slip conditions for hydrodynamically fully developed, single-phase laminar flow. The wall angles were  $57.4^\circ$  and  $45^\circ$ . They performed the 3-Dimensional numerical simulations using Finite-Volume approach method with various aspect ratios. The results obtained were summarized for thermally developing flow (TDF) with H1 boundary conditions. Using grids, they found that Local and average heat transfer coefficient in 3D channels at the entrance is proportional to  $(z^*)^{-1/2}$  which is

equivalent to 2D Graetz Leveque solutions. Through the numerical investigations, they found that changing aspect ratio  $\alpha$  or side wall angle  $\phi$  of channel affects both the Nussault number ( $Nu_{fd}$ ) and thermal entrance length ( $L^*_{th}$ ). **Stefano Nebuloni et al. [11]** conducted a numerical model of laminar annular film condensation for different channel shapes. Their statistical model is based on finite volume approach. Dimensional analysis and characteristic numbers were performed, and their simulation results were shown in both dimensional and dimensionless representations. From the numerical analysis Nussault number, liquid-vapor film thickness distribution, cross-sectional void fraction and mean vapour quality were obtained for different channels shapes. From analysis they found that, interfacial mass transfer phenomena and wall effects (disjoining pressure) results in a change in distribution of local heat transfer coefficient from 100 to 1000 kW/m<sup>2</sup>K.

**Mahshid Mohammadi et al. [12]** performed a numerical study on flow uniformity and pressure characteristics of amicrochannel array having triangular manifolds. In their study, the impact of geometry of right triangular manifold and dimensions of microchannel based on flow uniformity and pressure drop were investigated. The single phase steady-state laminar flow module in COMSOL Multiphysics 4.2 is used to perform CFD simulations having Reynolds number of ( $5 \leq Re \leq 25$ ). From the study, the results obtained entirely depends on the size of vertical corner spacing, an optimum corner angle through which the uniform flow distribution will be achievable. **Tu-chieh Hung et al. [13]** numerically studied the effects of enlarging the channel outlet on a porous microchannel heat sink (MCHS). The equations are solved numerically by the finite-volume Method. The heat transfer characteristics of parallel MCHSs with and without a porous medium were compared. The effects on the width and height enlargement ratios on the pressure drop, averaged Nussault number, heat transfer efficiency, thermal resistance were examined. The results showed that increasing the width or height expansion ratio reduces the pressure drop while thermal resistance is reduced with an enlarged channel outlet. **Mohammed H.A., [14]** performed numerical analysis of heat transfer enhancement using nanofluids in rectangular microchannel. They used the finite-volume method to solve the three-dimensional steady. The nanofluids considered were Ag, Al<sub>2</sub>O<sub>3</sub>, CuO, SiO<sub>2</sub>, and TiO<sub>2</sub> and their performance was compared with water. They found that the addition of nanoparticles increases the overall bulk temperature of cold fluids. They observed that SiO<sub>2</sub>nanofluid has the highest heat transfer coefficient, pumping power, shear stress among the other nanofluids.

Finally, it was concluded that Ag nanofluid has the highest effectiveness and performance index values followed by CuO, TiO<sub>2</sub>, Al<sub>2</sub>O<sub>3</sub>, water and eventually SiO<sub>2</sub>. **Yan Fan et al. [15]** manipulated the edge effect and temperature equalities on both planar and cylindrical heat surface for oblique finned microchannel. Numerical and experimental results were deviated by 6% for the temperature difference under all conditions. On their comparison, they found that cylindrical oblique finned heat sink has a nominal cooling solution for heat sources.

### 3. Effect of fluid flow through microchannel

#### 3.1 Experimental studies on various fluid flow

The selection of fluid plays a peculiar role in the performance of microchannel. However, the research and advancement in the design aspects of microchannel are in progress. Similarly, the research on fluid selection is also in the progressive status. The overall databases on the modes of fluid selection are stimulated on the basis of its developments. **Jacqueline B.Copetti et al. [16]** have performed experimental investigations on pressure drop and heat transfer coefficient by conducting the two-phase flow in a microchannel having a horizontal tube of 2.6mm ID. R134a was employed as the refrigerant. Heat flux and mass flux ranges between 10-100 kW/m<sup>2</sup> and 240-930 kg/m<sup>2</sup>s respectively. The experiment was conducted at two different saturation temperatures 12°C and 22°C. Nucleate Boiling is found to be the dominant mechanism. **Maxime Ducoulombier et al. [17]** carried out experimental investigation of flow boiling in single microchannel of Dia 0.529 mm with a horizontal stainless steel tube for three temperatures -10°C, -5°C, 0°C. Mass flux and heat flux are varying from 200 to 1200 kg/m<sup>2</sup>s and 10 to 30 kWm<sup>-2</sup> respectively. Flow patterns namely bubbly flow, elongated bubbly flow and annular flow was observed at Boiling number  $< 0.1$ ,  $BO > 1.1 \times 10^{-4}$ ,  $BO < 1.1 \times 10^{-4}$  respectively. The comparative study was conducted by **Jong-Taek Oh et al. [18]** who investigated heat transfer characteristics of two-phase flow in a horizontal stainless tube with ID 0.5, 1.5, and 3mm. R-22, R-134, R-410A, C<sub>3</sub>H<sub>8</sub>, CO<sub>2</sub> were used as working fluids with vapour quality of 1.0. Mass flux and heat flux were operated from 50-600 kg/m<sup>2</sup>s and 5-40 kWm<sup>-2</sup> respectively. They found evidently that CO<sub>2</sub> has higher heat transfer



coefficient. Finally, authors results gave 15.28% mean deviation and -0.48% average deviation for the correlation based on superposition model in small tubes.

**Fu. B.R et al. [19]** conducted an experimental study on heat transfer and Critical Heat Flux on ethanol-water mixtures in microchannel with artificial cavities. The test section was made of silicon strip having an inlet and outlet width of 215 and 1085 $\mu\text{m}$ . The divergence angle is  $1^\circ$ . Mass flux of 175  $\text{kg}/\text{m}^2\text{s}$  and heat flux ranges between 15.3 -1105  $\text{kW}/\text{m}^2$ . They had found that small addition of ethanol to water would significantly increase the Critical Heat Flux. The Mean Average Error of their CHF correlation is only 8.49% and more than 80% of experimental data are predicted within  $\pm 15\%$  error. Introduction of nanoparticles in fluids improve the flow performances. **TomioOkawa et al. [20]** carried out experiments to explore boiling heat transfer on to a hot stainless steel plate. The water drops containing the nanometre-sized titanium dioxide particles is used as a working fluid. They found that heat transfer coefficient is higher, when wall superheat is not too high. At low plate temperature, a large amount of liquid could remain on the surface to contribute cooling which increases the heat transfer coefficient. Both the results of pure water and the nanofluid are compared. **Maqbool M.H et al. [21]** investigated heat transfer characteristics of two-phase flow using ammonia in circular vertical microchannels made up of stainless steel. Mass fluxes from 100-500  $\text{kg}/\text{m}^2\text{s}$  were operated. Heat flux levels are 15 to 355  $\text{kW}/\text{m}^2$ . Saturation temperature of  $23^\circ\text{C}$ ,  $33^\circ\text{C}$  and  $43^\circ\text{C}$  are maintained.

They observed that, the heat transfer coefficient in 1.70mm tube is clearly dependent on heat flux in contrast to 1.224mm tube. For certain range of vapour fractions, heat transfer coefficient depends on heat flux and this effect is diminished at higher vapour fractions. **Xiumin Zhao et al. [22]** performed experimental investigation of flow boiling in horizontal micro-fin tube using  $\text{CO}_2$  as working fluid at saturation temperature of  $-30^\circ\text{C}$ . Test tube is made up of copper. Heat flux and mass flux varies from 10-25  $\text{kW}/\text{m}^2$  and 100-250  $\text{kg}/\text{m}^2\text{s}$  respectively. Outer and inner diameters are 7.94 and 7.31mm. They observed that at low vapour quality region ( $x < 0.05$ ), the flow boiling heat transfer coefficient shows a strong dependence on heat flux as per the power law [ $h_{\text{tp}} \sim q^n$ ]. The predictions from the empirical correlation disagree with the current experimental data with up to 50%. **Minxiali et al. [23]** conducted a flow boiling experiment in smooth horizontal tube with the internal diameter 2mm using a mixture of HFO1234yf and R32 as a working fluid. The mixtures are investigated at two mass fractions 80/20 and 50/50. The heat flux and mass flux ranges between 6-24  $\text{kW}/\text{m}^2$  and 100-400  $\text{kg}/\text{m}^2\text{s}$ . The evaporation temperature is  $15^\circ\text{C}$ . At various mass fractions, heat transfer coefficient are compared with pure HFO1234yf and pure R32. At 50% of mass fraction, heat transfer coefficient is greater than that of pure HFO1234yf.

**Zhaohui Liu et al. [24]** used kerosene kind hydrocarbon fuel as a working fluid for testing the heat transfer characteristics in an electrically heated horizontal tube with an inner diameter of 1.0mm. Heat flux: 20-1500  $\text{kW}/\text{m}^2$ , fluid temperature: 25-400 $^\circ\text{C}$ , mass flux: 1260-2160  $\text{kg}/\text{m}^2\text{s}$  and pressure: 0.25-25 Mpa. They found that the nucleate boiling is the dominant heat transfer mechanism. They kept the wall temperature constant during the FDSB of the non-azeotropic hydrocarbon fuel. Higher heat transfer coefficient was attained at higher fuel temperature. The expected higher heat flux and lower pressure helps to facilitate the heat transfer mode to approach the FDSB region. Excellent agreement was obtained between the predicted data and experimental data. **Matthew D. Byrne et al. [25]** conducted an experiment in microchannel for evaluating the thermal-hydraulic performance of CuO-nanofluids. Two factors were considered in this investigation. Solid media (CuO) concentration is considered as the first factor. The concentration values are 0.005%, 0.01% and 0.1%. Use of surfactant CTAB (Cetyltrimethyl Ammonium Bromide) as suspension enhancer is considered as the second factor. The nanofluid selection is made through the STEM and DLS techniques. Out of their six types of nanofluids which are tested, the larger increase in heat transfer is about 17% for a fluid with a concentration of 0.01% by volume. They have found clearly that use of surfactant is essential for maintaining a proper suspension of nanoparticles in the fluid.

**Akimaro Kawahara et al. [26]** experimentally investigated the effects of liquid properties in horizontal circular microchannel. Ethanol and distilled water were used as working fluids. They correlated the bubble velocity data with the drift flux model. Their analysis gave us a correlation of  $C_o$  (distribution factor) and  $F_L^2$  (two-phase friction multiplier) with some dimensionless number. The usage of nanofluids in the past few years are keep on increasing and the number of articles published on the basis of nanofluid usage is also dramatically increased. **Jacqueline Barber et al. [27]** gave a review on boiling heat transfer enhancement with nanofluids as nanoparticle deposition on the heating surface has considerably increased the heat transfer coefficient. The table 1 shows that various experimental study on microchannel heat sink.

**Table 1. Experimental data included in the consolidated database**

Author(s)	Channel Material	Dimensions (mm)	Fluid	G (kg/m <sup>2</sup> s)
JaquilineB.Copettie et al. [16]	Copper	D <sub>h</sub> =2.6	R134a	240-930
John Taek oh et al. [18]	Stainless steel	D <sub>h</sub> =0.5, 1.5, 3.0	R-22,R-134a R-410a, C <sub>3</sub> H <sub>8</sub> , Co <sub>2</sub>	50-600
MaximeDucoulombie et al. [17]	Stainless steel	D <sub>h</sub> = 0.529	Co <sub>2</sub>	200-1200
Chang Yong Park et al. [28]	Stainless steel	D <sub>h</sub> =0.061, 0.278	FC-72	189, 450
Arif B. Ozer et al. [29]	Aluminium	D <sub>h</sub> =0.229	R11	44
Sung-Min Kim et al. [30]	Copper	D <sub>h</sub> =0.175, 0.419	Water	670-5550
M.H Maqbool et al. [21]	Stainless steel	ID=1.70,1.224	Ammonia	100-500
Thanhtrung Dang et al. [31]	Aluminium	ID=0.375	Deionized water	250
Cheol Huh et al. [32]	Polydimethylsiloxane	D <sub>h</sub> =0.1035	Water	77.5, 154.9 and 309.8
H.Y. Wu et al. [33]	Silicon	D <sub>h</sub> =0.158, 0.082	Water	250
Melanie Derby et al. [2]	Copper	D <sub>h</sub> =0.424 to 0.839	R-134a	100-200
SylwiaSzcukiewicz et al. [4]	Copper	100 x 100 mm <sup>2</sup>	R245fa,R236fa, and R1234ze	283-2370
AymanMegahed et al. [6]	Silicon	D <sub>h</sub> =0.248	FC-72	99-290
Ahmad Odaymet et al. [5]	Silicon	D <sub>h</sub> =0.305	Water	14-31
Yuan Wang et al. [7]	Borosilicate glass	D <sub>h</sub> =0.1	FC-72	11.2,22.4 4.8
TannazHarirchian et al. [8]	Silicon/Pyrex sheet	12.75 x 1.05	FC-77	225–1420
Boye H et al. [34]	Nickel alloy	D <sub>h</sub> =1.50	Water	50-100
Bogojevic D. et al. [35]	Silicon	D <sub>h</sub> =0.194	Deionized water	71-204
FarzadHoushmand et al. [36]	Silicon/Pyrex	27.5 x 1.5	Deionized water	13-54 ml/min
Fanghao Yang et al. [37]	Silicon/Nano-wired	0.2 x 0.25	Deionized water	404
Susan N. Ritchey et al. [38]	Silicon	12.7 x 12.7	FC-77	890
Tannaz Harirchian et al. [39]	Silicon	12.7 x 12.7	Fluorinert FC-77	250 to 1600
Yong Jiun Lee et al. [40]	Silicon	12.7 x 12.7	De-ionized water	100 to 500
Li Xu et al. [41]	Pyrex glass / Silicon wafer	7.5 x 0.1 x 0.25	Pure water and nanofluid	171, 285 and 401
DongYao Liu et al. [42]	Silicon	D <sub>h</sub> =0.293	Water	11.09 to 44.36
Morshed A.K.M.M. et al. [43]	Copper	D <sub>h</sub> =0.672	De-ionized water	-
Daxiang Deng et al. [44]	Oxygen-free pure Copper	D <sub>h</sub> =0.776	deionized water and ethanol	200–300
Chun Ting Lu et al. [45]	Copper	D <sub>h</sub> =0.120	Water	99 to 297

### 3.2 Numerical studies on various fluid flow

**DorinLelea [46]** performed numerical modeling of heat transfer and fluid flow using  $\text{Al}_2\text{O}_3/\text{Water}$  in a square microchannel with a hydraulic diameter of  $50 \mu\text{m}$  and heat flux  $q=35 \text{ W/m}^2$ . The volume concentration of nanofluid varies from 1-9%. Various diameters were taken. They resulted in that heat transfer coefficient increases with an increase in particle size. Their model revealed that heat transfer performance is higher for the heating case than in the cooling case. They concluded that heat transfer coefficient is under-estimated for 305 in case of cooling and over-estimated 20% for heating case. **Ganapathy H et al. [47]** proposed a numerical model for the analysis of condensation heat transfer and fluid flow characteristics in single microchannel. A microchannel dimension of  $100 \mu\text{m}$  was modelled using a 2-D Computational domain. Working fluid is R134a; Mass flux:  $245\text{-}615 \text{ kg/m}^2\text{s}$ ; Heat flux:  $200\text{-}800 \text{ KW/m}^2$ . They compared the two-phase frictional pressure drop and two-phase nussault number against the numerical empirical correlations in the literature. The two-phase pressure drop was predicted with 8.1% of MAE of approach in the literature. From their validated results, we came to know that numerical simulations will be having the better accuracy towards the condensation heat transfer.

**Mat Tokitet al. [48]** analysed the thermal performance of optimised interrupted microchannel heat sink using nanofluids with  $n_c=3$ . The particle diameter they took are  $30 \text{ nm}$  to  $60 \text{ nm}$ ; Nanofluid is of type  $\text{Al}_2\text{O}_3$ ,  $\text{CuO}$  and  $\text{SiO}_2$  at Reynold's number is ranging from  $140\text{-}1034$ . They found that IMCHS have the highest nussault number than conventional MCHS, but there was a slight increase in pressure drop as in the case of IMCHS.  $\text{Al}_2\text{O}_3$  had a high thermal performance when compared with  $\text{CuO}$  and  $\text{SiO}_2$ .  $\text{SiO}_2$  stands last in thermal augmentation. They concluded that, when nanoparticle diameter increases, nussault number increases and vice-versa. **Yue-Tzu Yang [49]** presented a numerical study on trapezoidal microchannel heat sink using  $\text{CuO}/\text{Water}$  as nanofluid. Using finite volume method energy equations are discretized. They compared the CFD predictions of laminar and turbulent flow for both the single and two-phase flow. In addition to the flow, they compared the thermal resistance of both the phase models. Their numerical results showed that large temperature difference between MCHS inlet and outlet is obtained when  $V=10 \text{ mL/min}$  and  $F=0.4\%$ . Their predictions help us in concluding that two-phase flow is more accurate than single phase model.

**Mohammad Kaltehet al. [50]** conducted experimental and numerical study on alumina-water nanofluid in a rectangular microchannel heat sink. A two-phase Eulerian- Eulerian method using finite volume approach was adopted in that study. Velocity and temperature profiles for two-phase results are higher than the pure water. For nanofluid flow two-phase flow finds good agreement with experimental results. The maximum deviation from experimental results are  $12.61\%$  and  $7.42\%$  for single phase flow. **Manu Mital [51]** evaluated the heat transfer improvement of a nanofluid heat sink with developed laminar flow convection. Their model used semi-empirical correlations to calculate the nanofluid's thermo-physical properties. Their model help us to find the necessary design variables. They considered volume fraction as the most significant factor in impacting the heat transfer coefficient. Their results show that heat transfer coefficient is maximum at smallest possible particle diameter. The table 2 shows that various numerical correlations for Nussault number and heat transfer coefficient on microchannel heat sink.

**Table 2. Numerical correlations for Nussault number and heat transfer coefficient**

Authors	Correlations	Remarks
John P.Mchal et al. [10]	$h(z) = \frac{\sum_{XY} q''(x, y, z) dA(X, Y, Z)}{\sum_{XY} [T_W(x, y, z) - T_m(z)] dA(x, y, z)} Nu_{avg}(z)$ $= \left(\frac{D_h}{K_f}\right) h_{avg} = \left[\frac{1}{Z^*} \sum \frac{1}{Nu_z} dz^*\right]^{-1}$	$D_h=100\mu\text{m}$ , Water, Steady state incompressible, laminar flow
Stefano Nebuloni et al. [11]	$h(z) = \frac{k_f}{T^W - T^S} \frac{1}{P} \int_P^L \frac{\partial T}{\partial n} I_W dl$	$D_h=10 \mu\text{m} - 3\text{mm}$ , R134, ammonia; condensation



Li Zhuo et al. [52]	$h(z) = \frac{\overline{q_s}, r(z)}{\Delta T_z} Nu_{z,ave} = \frac{h_{z,ave} \cdot D}{k_1}$	Re=100, triangular and rectangular; laminar flow
DorinLelea et al. [46]	$h_{ave} = \frac{q/r}{t_w/r}$	$D_h=50 \mu\text{m}$ , $\text{Al}_2\text{O}_3/\text{Water}$ , $d_p=13,28,47 \text{ mm}$
Ganapathi H et al. [47]	$h_{tp} = \frac{q''}{T_{sat} - T_{wall}}$ $Nu_{tp} = \frac{h_{tp} D}{k_L}$	$D_h=100 \mu\text{m}$ , R134, Condensation, MAE = 8.1%
RabienatazDarzi A.A. et al. [53]	$Nu = \frac{q'' d}{k_{ef}(T_w - T_b)}$	Re=10000-40000, Water/ $\text{Al}_2\text{O}_3$ , Turbulent flow
Mohammed Kalteh et al. [50]	$\bar{h} = \frac{Q}{A_h \Delta T_m}$ $\overline{Nu} = \frac{\bar{h} D_h}{k_l}$	$\text{Al}_2\text{O}_3$ , Rectangular (94.3mm x 28.1mm x 580 $\mu\text{m}$ ), laminar
Manu mital et al. [51]	$h_x = \frac{K_{nf} Na_x}{D}, h_{avg} = \frac{1}{L} \int_0^L h_x dx$	$D_H=0.1 \text{ mm}$ , nanofluid, laminar-incompressible flow
Yan fan et al. [54]	$h_x = \frac{q_s''}{T_s - T_\infty} = X^{-0.5} \frac{K d\theta}{2dn} \sqrt{\frac{u_\infty}{\gamma}}$ $Nu_{ave,fd} = h_{ave,fd} \frac{D_h}{K}$	Oblique angle= 20- 45°, Reynolds number= 20-900. Nessault number deviation= -5.8% to 7.0%
ErcanM.Dede et al. [55]	$h_{exp} = \frac{q_{app} f_{eff}}{A_d [T_s - T_{f-in}]}$ $h_{sim} = \frac{q''_{local}}{T_s - T_{f-in}}$	Flow condition= 1070 < Re < 6370, ethylene glycol/Water
Artemov V. I. et al. [56]	$Nu = \frac{q_w d_h}{l(t_{wex} - t_{ex})}$	$D_H= 10 \mu\text{m}$ to 1mm, Six rectangular channels, Laminar flow, (Re < 10 <sup>3</sup> , Pe > 10 <sup>2</sup> )
Yongping Chen et al. [57]	$\overline{Nu} = \frac{\int_{L_e}^L Nu_x dx}{L - L_e}$	H = 100 $\mu\text{m}$ , L = 5 cm, Cantor set structure, Steady laminar flow.

## 4. Flow boiling

### 4.1 Experimental studies on flow boiling

The traditional heat removal systems cannot meet the requirement of inlet heat fluxes which are more than the 100 W/cm<sup>2</sup>. Since there was a smaller pressure drop at this stage, electronic devices are in the need of the newer method for heat removal process. Apart from the pool boiling and convective boiling, flow boiling stepped into the channels to give the enhanced performance. Double layered microchannel **Gongnan Xie et al. [58]** with flow boiling also gave a better performance. **Fangio Yang et al. [59]** conducted an experimental study on flow boiling with Deionized water in Silicon (Si) Microchannels. The average heat transfer coefficient (HTC) and critical heat factor (CHF) were enhanced by up to 32.6% and 31.7% of mass flux of 389kg/ m<sup>2</sup>s, respectively. The comparison between obtained HTC and CHF values with flow boiling in Microchannels having Inlet restrictions (IR<sub>s</sub>) was made. They found that HTC of flow boiling in single annular flow was increased up to 2.48% while CHF in new boiling regime was 6.4-25.8% lower. Based on above values, Results showed that a single flow boiling regime were the fundamental reasons behind the significant heat transfer

enhancements during flow boiling. **Bogojevic D et al. [35]** were experimentally investigated on bubble dynamics and effect on the flow boiling instabilities and heat transfer in a Multiple Microchannel heat sink. The heat sink used by them containing 40 parallel Rectangular channels, having hydraulic diameter of 194 $\mu\text{m}$  and aspect ratio of 0.549 with deionised water as working fluid at 71 $^{\circ}\text{C}$  inlet temperature. Then the effects of heat and mass flux on bubble growth rate, bubble growth period, departure diameter and the phase alteration between liquid, vapor and two-phase flow were observed and analysed. The increase in heat flux results in a decrease of liquid film thickness from 25 $\mu\text{m}$  to 15 $\mu\text{m}$  and the Confinement of Microchannels lead to the unique Bubble Dynamics along the channels.

**Boye H et al. [34]** studied the flow boiling heat transfer characteristics similar to previously discussed journal [4]. Here the circular channel with 3bar inlet pressure and heat flux of 10 to 115 $\text{KW}/\text{m}^2$  was maintained. The results are similar to that of journal [4] along with two boiling mechanisms such as Nucleate boiling and convective boiling. **Carlo Bartoli et al. [60]** made use of ultrasonic waves in 2010 to enhance the heat transfer. They selected the sub-cooled boiling regime as it suits well for the heat transfer enhancement. 45 $^{\circ}$  to 10 $^{\circ}\text{C}$  were the cooling degrees chosen by them. The conditions in which the enhancement takes place are at  $f=40\text{kHz}$ ,  $P_{\text{gen}}=500\text{W}$  and heat flux =  $1.2 \times 10^5 \text{ W}/\text{m}^2$ . Using ultrasonic waves heat transfer has enhanced up to 62%. **Farzad Houshmand et al. [61]** had done an experimental investigation on bubble formation process in the presence of Micro-pillar by injecting a Gas stream into a Microchannel at varying Slit angles with respect to liquid flow. Three different bubble formation modes such as discrete bubbling mode, attached ligament mode and mixed mode was found. Here the injection mode affects the characteristics of formation mode such as coalescence and bubble ejection. Both these have an effect on bubble size and frequency. From this, they came to know the injection angle has a significant impact on mixing characteristics of bubbles ejected from Micro pillar in the flow. **Susan N. Ritchey et al. [38]** performed experiments on flow boiling phenomena in a Microchannel heat sink with Hotspots as well as non-uniform Streamwise & transverse high heating conditions spanning across the entire heat sink area. Microchannel with a 5\*5 array of separate controllable heaters are attached to 12.7mm\*12.7mm square base with Dielectric fluorinert liquid FC-77 as a fluid with mass flux of 890 $\text{kg}/\text{m}^2\text{s}$ . The effects of non-uniform hot spots, heating profiles in a Microchannel heat sink, Wall temperature & location of boiling at beginning stage were investigated. Also based on obtained results, it was evidently come to know that for a fragile Substrate significant lateral conduction occurs in the heat sink base.

**Fanghao Yang et al. [59]** reported that pressure drop was reduced by almost 48% and critical heat flux was increased by approximately 300% in SiNW channels, compared with small wall Microchannels. Through the systematic study, they found that the separated vapor, liquid flows and flattened liquid-vapor interfaces under the single annular flow are the primary reason for ~48% reduction in pressure drop. At last they concluded that hydraulic characteristics of single annular flow were systematically investigated to reveal the mechanisms responsible for reduced pressure drop and enhanced Critical heat flux (CHF). **Woorim Lee et al. [62]** studied numerically on boiling heat transfer and bubble growth rate on a microchannel using conservation equation of mass, momentum and energy. The method of sharp - interface level- set was tracked to determine the bubble-shape. The numerical results demonstrated that micro finned surface could enhance boiling that transfer by about 40-60% compared to the plane surface. The design aspects fin arrangement are optimized in which the optimal fin spacing and height are about  $0.6D_{b,0}$  and  $0.2D_{b,0}$ .

#### 4.2 Numerical studies on flow boiling

**Rui Zhuan et al. [63]** simulated on bubble behavior of flow boiling for the fluid R-134a and R22 in 0.50 mm circular channel whose mass velocities ranges between 350  $\text{kg}/\text{m}^2\text{s}$  – 2000 $\text{kg}/\text{m}^2\text{s}$ . Simulation of two-phase flow was carried out by VOF method. The frequency of bubble generation was calculated by the relation  $f = (\delta_{\text{cpl}} T_{\text{sat}}) / (\delta h_{\text{lu}} R_{\text{dp}})$ . It was seen that the decrease in saturation temperature increases the surface tension of the liquid and bubble coalescence readily. At the same thermal condition, bubble growth and lifting size in R-22 are lower than that of an R-134a and it was indicated that the peak bubble frequency appears in bubbly/slag flow region. **Mushtaq I. Hasan et al. [64]** carried out a numerical simulation to solve the 3D developing flow and 3D conjugate heat transfer of balanced counter flow. Microchannel Heat Exchanger a was tested for various cross-sections such as trapezoidal, iso-triangular, rectangular, square and circular. When numbers of channels are increased, there will be increase in both effectiveness and pressure drop. Finally, they came to the conclusion that circular channels gave best thermal and hydraulic performance when compared with other sections.

**IssamMudhwar [65]** examined the characteristics of pressure drop in sub-cooled two-phase microchannel heat sink. Flow characteristics are predicted by using conservation equation like mass, momentum & energy control volume for the thermodynamics equilibrium below zero, by incorporating this relation model by developing homogeneous layer. This was constructed specifically for developing subcooled flow boiling and this model enables the determination of axial variation in two-phase layer thickness & velocity. It is then compared with HFE-7100 pressure drop data for microchannel diameter of 176-416  $\mu\text{m}$ , mass velocity of 670-5550  $\text{kg/m}^2\text{s}$  & inlet temperature of 0 $^\circ\text{C}$  & -30 $^\circ\text{C}$ , pressure drop is predicted with a mean absolute of 14.9%. **Magnini M et al. [66]** investigated sequential bubbles on slug flow boiling within microchannel. Simulations are performed by means of fine volume commercial CFD solver, ANSYS FLUENT release 12.1 and VOF is adopted for numerical data of liquid-vapour interface. It was noticed that the liquid slugs which separates the bubbles is shorter than this region & thus the trailing bubble exhibited due to different evaporation rates. They assumed the contribution of the liquid slug zone to the overall heat transfer performance were comparable to that of the liquid film region for the present working condition. **Naviraju Kupusamy et al. [67]** has employed a numerical study of a conjugate 3D compilation to study the laminar convective heat transfer in MASP. Computational grids for both solid and fluid regions were generated using hex-map scheme in GAMBIT V2.11. The standard simple algorithm is employed for pressure-velocity coupling method. They evidently found that thermal performance increases with an increase in the secondary pressure due to which diversion in mainstream channel results in greater fluid transfer. **Woorim Lee et al. [68]** compared the plain and micro finned surface by solving the conservation equations of mass, momentum and energy. sharp-interface level-set method is used to track the bubble shape. Their results showed that micro finned surface transfer 40 – 60% of heat when compared with plain surface. **Sarangi R.K et al. [69]** developed the two numerical models assuming homogeneous and annular flow boiling. Grass-root level method is used to solve the governing equations. The governing equation predictions are compared with two experimental data. Their results gave us a prediction that annular flow model have higher pressure drop than homogeneous model. In addition to their results, they found that non-uniform heating would give a better result over fluid dynamics and heat transfer.

## 5. Study on oblique finned microchannel

**Tannaz Harirchian et al. [70]** had studied the Flow Regime map with phase change number and newly projected on Convective confinement number as the coordinates. Flow regime based models for prediction of heat transfer coefficient in slug flow & annular/wispy annular flow are developed & compared to experimental data. The Mean Average Error for various flow regions such as bubbly flow, annular flow, annular/wispy flow and slug flow is 13.9%, 17.3%, 21.8% and 17.8% respectively are obtained. They found the Regime-based prediction of pressure drop resulted in much better agreement with experiments. **Yan fanet al. [54]** proposed a novel oblique finned microchannel to fit over cylindrical heat sources in the form of an enveloping jacket with copper as a test piece material. Reynolds number varied from 50-500. Numerical and experimental comparisons between its cooling effectiveness and conventional straight fin MCHS were done. The numerical results showed that  $\text{Nu}_{\text{ave}}$  for the cylindrical oblique finned MCHS increases up to 75.6% and thermal resistance decreased up to 59.1%. Based on this, they concluded that the heat transfer is higher for cylindrical oblique finned microchannel. **Yuan wang et al. [7]** studied the effects of channel hydraulic diameter, vapour quality and heat flux of the flow boiling heat transfer with high aspect ratio. The mass fluxes utilized were 11.2, 22.4 and 44.8  $\text{kgm}^{-2}\text{s}^{-1}$ . Heat fluxes ranges from 0-18.6  $\text{KWm}^{-2}$  with FC-72 as fluid with channel hydraulic diameters of 571, 762 and 1454  $\mu\text{m}$  for aspect ratios 20, 20 and 10 respectively. The critical heat flux (CHF) increases with an increase in channel diameter and temperature overshoot is observed at onset boiling (ONB). From the study, the results clearly show that local heat transfer coefficient increases when hydraulic diameter is decreased. **K.Balasubramanian et al. [71]** examined the pressure drop and flow boiling heat transfer in straight and expanding microchannel with similar dimensions. Deionised water was used as a fluid and test piece are made of copper with the area of 25mm x 15mm. They also used the microchannel containing the nominal width of 30  $\mu\text{m}$  and aspect ratio of 4 by wire cut electro-discharge machining process. Their investigation shows that the expanded microchannel requires lesser pumping power to drive the fluid when compared with a straight microchannel and also the heat transfer performance is higher in microchannels.

## 6. Conclusion

The conceptual reviews of various authors give a clear-cut idea of improvising the microchannel design aspects of two-phase flow boiling. This referential paper shows the era of development of experimental

and numerical approach of various aspects such as a cross-section, fluids selection and flow boiling. Even though many articles have been published under this category, we are still in a phase to attempt a better understanding of their flow patterns and fluid flow characteristics.

The consolidated discussions on various aspects are summarized.

1. This paper completely reviewed the fluids, cross section and types of fins implemented in microchannel heat sink in both the experimental and numerical manner. Numerical correlations for heat transfer and nussault number for various fluid flow were also tabulated
2. It also discussed the oblique fin which is obtained by the segmentation of continuous fin into oblique sections. Insight to that, based on the flow boiling aspects, various flow patterns, bubble growth rate, and pressure drop characteristics in oblique finned microchannel are discussed.
3. Based on the consolidated databases from the review, two-phase flow boiling can be performed in an oblique finned microchannel with different channel cross section such as square, semicircular and trapezoidal. Microchannel of different channel cross sections with oblique cuts can be developed. Flow boiling investigations can be carried out for various flow rates and Reynolds number. The heat and flow characteristics can be accomplished.

### Nomenclature

A	Area (m <sup>2</sup> )	<b>Greek symbol</b>	
Co	Distributor factor	$\Gamma$	surface tension (N/m)
D <sub>h</sub>	Hydraulic diameter (m)	$\Theta$	contact angle
d, D	Diameter (m)	$\alpha$	void fraction
F <sub>L</sub>	Two phase friction multiplier	$\mu$	viscosity (kg/(sm))
E	Energy (kJ)	$\rho$	density (kg/m <sup>3</sup> )
G	Gravity (kg/s)	$\tau$	contraction ratio
H	heat transfer coefficient (W/m <sup>2</sup> K)		
L <sub>th</sub>	thermal entrance length (m)	<b>subscripts</b>	
K	thermal conductivity (W/m K)	eff	effective
L	length (m)	exp	experimental
Nu	nusselt number	sat	saturation
P	power (W)	w	wall
P	pressure (Pa)	ze	error
q	heat flux (W/m <sup>2</sup> )		
Re	Reynolds number		
r, R	radius of bubble (m)		
T	temperature (0C)		
t	time (s)		
V	volume(m <sup>3</sup> )		
X	vapour quality		

### References

1. Jingru Zhang, Po Ting Lin, Yogesh Jaluria. Design and Optimization of Multiple Microchannel Heat Transfer Systems. Journal of Thermal Science and Engineering Applications., 2014, Vol: 6 / 011004-1.
2. Melanie Derby, HeeJoon Lee, YoavPeles, Michael K. Jensen. Experimental thermal-hydraulic evaluation of CuO nanofluids in microchannels at various concentrations with and without suspension enhancers. International Journal of Heat and Mass Transfer., 2012,55: 2684–2691.
3. Tu-Chieh Hung, Wei-Mon Yan, Wei-Ping Li. Analysis of heat transfer characteristics of double-layered microchannel heat sink. International Journal of Heat and Mass Transfer., 2012,55:3090–3099.
4. SylwiaSzcukiewicz, NavidBorhani, John Richard Thome. Two-phase heat transfer and high-speed visualization of refrigerant flows in 100 100 mm<sup>2</sup> silicon multi-microchannels. International journal of refrigeration., 2012, 1: 1-12.

5. Ahmad Odaymet, HasnaLouahlia-Gualous. Experimental study of slug flow for condensation in a single square microchannel. *Experimental Thermal and Fluid Science.*, 2012,38: 1–13.
6. AymanMegahed, Experimental investigation of flow boiling characteristics in a cross-linked microchannel heat sink. *International Journal of Multiphase Flow.*, 2011,37:380–393.
7. Yuan Wang, KhellilSefiane. Effects of heat flux, vapour quality, channel hydraulic diameter on flow boiling heat transfer in variable aspect ratio micro-channels using transparent heating. *International Journal of Heat and Mass Transfer.*, 2012, 55:2235–2243.
8. Tannaz Harirchian, Suresh V Garimella. Effects of channel dimension, heat flux, and mass flux on flow boiling regimes in microchannels. *International Journal of Multiphase Flow.*, 2009,35:349–362.
9. Talimi V, Muzychka Y.S, Kocabiyik S. A review on numerical studies of slug flow hydrodynamics and heat transfer in microtubes and microchannels. *International Journal of Multiphase Flow.*, 2012,39:88–104.
10. John P. McHale, Suresh V Garimella. Heat transfer in trapezoidal microchannels of various aspect ratios. *International Journal of Heat and Mass Transfer.*, 2010, 53: 365–375.
11. Stefano Nebuloni, John R. Thome. Numerical modeling of laminar annular film condensation for different channel shapes. *International Journal of Heat and Mass Transfer.*, 2010,53: 2615–2627.
12. MahshidMohammadia, Goran N. Jovanovicb, Kendra V. Sharpa. Numerical study of flow uniformity and pressure characteristics within a microchannel array with triangular manifolds. *Computers and Chemical Engineering.*, 2013,52:134– 144.
13. Tu-Chieh Hung, Yu-Xian Huang, Wei-Mon Yan. Thermal performance of porous microchannel heat sink:Effects of enlarging channel outlet. *International Communications in Heat and Mass Transfer.*, 2013,48: 86–92.
14. Mohammeda H.A, Bhaskaran G, Shuaib N.H, R.Saidur. Numerical study of heat transfer enhancement of counter nanofluids flow in rectangular microchannel heat exchanger. *Superlattices and Microstructures.*, 2011,50: 215–233.
15. Yan Fan, Poh Seng Lee, Beng Wah Chua. Investigation on the influence of edge effect on flow and temperature uniformities in cylindrical oblique-finned minichannel array. *International Journal of Heat and Mass Transfer.*, 2014,70: 651–663.
16. Jacqueline B Copetti, Mario H Macagnan, Flavia Zinani, Nicole L.F Kunsler. Flow boiling heat transfer and pressure drop of R-134a in a mini tube, An experimental investigation. *Experimental Thermal and Fluid Science.*, 2011,35:636–644.
17. Maxime Ducoulombier, Stephen Colasson, Jocelyn Bonjour, Philippe Habeschill. Carbon dioxide flow boiling in a single microchannel – Part II: Heat transfer. *Experimental Thermal and Fluid Science.*, 2011,35: 597–611.
18. Jong-Taek Oh, Pamitran A.S, Kwang-II Choi, PegaHrnjak. Experimental investigation on two-phase flow boiling heat transfer of five refrigerants in horizontal small tubes of 0.5, 1.5 and 3.0 mm inner diameter. *International Journal of Heat and Mass Transfer.*, 2011,54: 2080–2088.
19. Fu B.R, Tsou M.S, Chinpan. Boiling heat transfer and critical heat flux of ethanol–water mixtures flowing through a diverging microchannel with artificial cavities. *International Journal of Heat and Mass Transfer.*, 2012,55:1807–1814.
20. TomioOkawa, Kenta Nagano. Boiling heat transfer during single nanofluid drop impacts onto a hot wall. *Experimental Thermal and Fluid Science.*, 2012,36: 78–85.
21. Maqbool M.H, Palm B, Khodabandeh R. Boiling heat transfer of ammonia in vertical smooth mini channels: Experimental results and predictions. *International Journal of Thermal Sciences.*, 2012, 54:13-21.
22. Xiumin Zhao, PradeepBansal. Flow boiling heat transfer analysis of new experimental data of CO<sub>2</sub> in a micro-fin tube at 30° C. *International Journal of Thermal Sciences.*, 2012,59:38-44.
23. MinxiaLi, Chaobin Dang, EijiHihara. Flow boiling heat transfer of HFO1234yf and R32 refrigerant mixtures in a smooth horizontal tube: Part I. Experimental investigation. *International Journal of Heat and Mass Transfer.*, 2012,55:3437–3446.
24. Zhaohui Liu, Qincheng Bi, Yong Guo, Qianhua. Heat transfer characteristics during subcooled flow boiling of a kerosene kind hydrocarbon fuel in a 1 mm diameter channel. *International Journal of Heat and Mass Transfer.*, 2012,55:4987–4995.
25. Matthew D. Byrne, Robert A. Hart, Alexandre K. da Silva. Experimental thermal–hydraulic evaluation of CuOnanofluids in microchannels at various concentrations with and without suspension enhancers. *International Journal of Heat and Mass Transfer.*, 2012,5: 2684–2691.

26. Akimaro Kawahara, Michio Sadatomi, Keitaro Nei, Hideki Matsuo. Experimental study on bubble velocity, void fraction and pressure drop for gas-liquid two-phase flow in a circular microchannel. *International Journal of Heat and Fluid Flow.*, 2009,30:831–841.
27. Jacqueline Barber, David Brutin, Lounes Tadrist. A review on boiling heat transfer enhancement with nanofluids. *Nanoscale Research Letters.*, 2011, 6:280.
28. Chang Yong Park, Yonghee Jang, Bosung Kim, Yongchan Kim. Flow boiling heat transfer coefficients and pressure drop of FC-72 in micro channels. *International Journal of Multiphase Flow.*, 2012,39:45–54.
29. Arif B Ozer, Ahmet F Oncel, Keith Hollingsworth D, Larry C Witte. A method of concurrent thermographic–photographic visualization of flow boiling in a midi channel. *Experimental Thermal and Fluid Science.*, 2011,35:1522–1529.
30. Sung-Min Kim, Issam Mudawar. Consolidated method to predicting pressure drop and heat transfer coefficient for both subcooled and saturated flow boiling in micro-channel heat sinks. *International Journal of Heat and Mass Transfer.*, 2012,55:3720–3731.
31. Thanhtrung Dang, Jyh-tong Teng, Jiann-cherng Chu. A study on the simulation and experiment of a microchannel counter-flow heat exchanger. *Applied Thermal Engineering.*, 2010,30: 2163-2172.
32. Cheol Huh, Moo Hwan Kim. An experimental investigation of flow boiling in an asymmetrically heated rectangular micro channel. *Experimental Thermal and Fluid Science.*, 2006,30:775–784.
33. Wu H.Y, Ping Cheng. Visualization and measurements of periodic boiling in silicon microchannels. *International Journal of Heat and Mass Transfer.*, 2003, 46:2603–2614.
34. Boye H, Staate Y, Schmidt J. Experimental investigation and modelling of heat transfer during convective boiling in a minichannel. *International Journal of Heat and Mass Transfer.*, 2007,50: 208–215.
35. Bogojevic D, Sefiane K, Duursma G, Walton A.J. Bubble dynamics and flow boiling instabilities in microchannels. *International Journal of Heat and Mass Transfer.*, 2013, 58: 663–675.
36. FarzadHoushmand, Daren Elcock, Michael Amitay, YoavPeles. Bubble formation from a micropillar in a microchannel. *International Journal of Multiphase Flow.*, 2014,59:44–53.
37. Fanghao Yang, Xianming Dai, YoavPele, Ping Cheng, Jamil Khan, Chen Li. Flow boiling phenomena in a single annular flow regime in microchannels (II): Reduced pressure drop and enhanced critical heat flux. *International Journal of Heat and Mass Transfer.*, 2014, 68: 716–724.
38. Susan N Ritchey, Justin A Weibel, Suresh V Garimella. Local measurement of flow boiling heat transfer in an array of non-uniformly heated microchannels. *International Journal of Heat and Mass Transfer.*, 2014,71: 206–216 .
39. Tannaz Harirchian, Suresh V Garimella. Microchannel size effects on local flow boiling heat transfer to a dielectric fluid. *International Journal of Heat and Mass Transfer.*, 2008,51: 3724–3735.
40. Yong Jiun Lee, Pawan K Singh, Poh Seng Lee. Fluid flow and heat transfer investigations on enhanced microchannel heat sink using oblique fins with parametric study. *International Journal of Heat and Mass Transfer.*, 2015,81: 325–336.
41. Li Xu, Jinliang Xu. Nanofluid stabilizes and enhances convective boiling heat transfer in a singleMicrochannel. *International Journal of Heat and Mass Transfer.*, 2012,55: 5673–5686.
42. DongYao Liu, Xia Wenga, XiaoGuang Xu. Experimental study on the heat transfer coefficient of water flow boiling in mini/microchannels. *Experimental Thermal and Fluid Science.*, 2011,35:1392–1397.
43. Morshed, Fanghao A.K.M.M.Yang, Yakut Ali M, Jamil A. Khan, Chen Li. Enhanced flow boiling in a microchannel with integration of nanowires. *Applied Thermal Engineering.*, 2012,32: 68-75.
44. Daxiang Deng, Wei Wana, Yong Tang, Zhenping Wanc, Dejie Liang. Experimental investigations on flow boiling performance of reentrant and rectangular microchannels – A comparative study. *International Journal of Heat and Mass Transfer.*, 2015,82:435–446.
45. Chun Ting Lu, Chin Pan. Convective boiling in a parallel microchannel heat sink with a diverging crosssection and artificial nucleation sites. *Experimental Thermal and Fluid Science.*, 2011,35: 810–815.
46. DorinLelea. The performance evaluation of Al<sub>2</sub>O<sub>3</sub>/water nanofluid flow and heat transfer in microchannel heat sink. *International Journal of Heat and Mass Transfer .*, 2011,54: 3891–3899.
47. Ganapathy H, Shoostari A, Choo K, Dessiatoun S, Alshehhi M, Ohadi M. Volume of fluid-based numerical modeling of condensation heat transfer and fluid flow characteristics in microchannels. *International Journal of Heat and Mass Transfer.*, 2013,65: 62–72.



48. Mat Tokit E, Mohammed H.A, Yusoff M.Z. Thermal performance of optimized interrupted microchannel heat sink (IMCHS) using nanofluids. *International Communications in Heat and Mass Transfer.*, 2012,39: 1595 -1604.
49. Yue-Tzu Yang, Kuo-Teng Tsai, Yi-Hsien Wang, Shih-Han Lin. Numerical study of microchannel heat sink performance using nanofluids. *International Communications in Heat and Mass Transfer.*, 2014,57: 27–35.
50. Mohammad Kalteh, Abbas Abbassi, Majid Saffar-Avval, Arjan Frijns, Anton Darhuber, Jens Harting. Experimental and numerical investigation of nanofluid forced convection inside a wide microchannel heat sink. *Applied Thermal Engineering.* , 2012,36: 260-268.
51. Manu Mital. Analytical analysis of heat transfer and pumping power of laminar nanofluid developing flow in microchannels. *Applied Thermal Engineering.*, 2013,50: 429-436.
52. Li Zhuo, Tao Wen-Quan, He Ya-Ling. A numerical study of laminar convective heat transfer in microchannel with non-circular cross-section. *International Journal of Thermal Sciences.*, 2006,45: 1140–1148.
53. Rabienataj Darzi A.A, Mousa Farhadi, Kurosh Sedighi, Shahriar Aallahyari, Mojtaba Aghajani Delavar. Turbulent heat transfer of Al<sub>2</sub>O<sub>3</sub>–water nanofluid inside helically corrugated tubes: Numerical study. *International Communications in Heat and Mass Transfer.*, 2013,41: 68–75.
54. Yan Fan, Poh Seng Lee, Li-Wen Jin, Beng Wah Chua. A simulation and experimental study of fluid flow and heat transfer on cylindrical oblique-finned heat sink. *International Journal of Heat and Mass Transfer.*, 2013,61: 62-72.
55. Ercan M. Dede, Yan Liu. Experimental and numerical investigation of a multi-pass branching microchannel heat sink. *Applied Thermal Engineering.*, 2013,55:51-60.
56. Artemov V I, Leontiev A I, Polyakov A F. Numerical Simulation of Convection-Conduction Heat Transfer in a Block of Rectangular Microchannels. *Russian Academy of Sciences and Springer Science + Business Media, Inc, High Temperature.*, 2005,43: 580–594.
57. Yongping Chen, Panpan Fu, Chengbin Zhan, Mingheng Shi. Numerical simulation of laminar heat transfer in microchannels with rough surfaces characterized by fractal Cantor structures. *International Journal of Heat and Fluid Flow.*, 2010,31: 622–629.
58. Gongnan Xie, Yanquan Liu, Bengt Sundén, Weihong Zhang. Computational Study and Optimization of Laminar Heat Transfer and Pressure Loss of Double-Layer Microchannels for Chip Liquid Cooling. *Journal of Thermal Science and Engineering Applications.*, 2013, DOI: 10.1115/1.4007778.
59. Fanghao Yang, Xianming Dai, Yoav Peles, Ping Cheng, Jamil Khan, Chen Li. Flow boiling phenomena in a single annular flow regime in microchannels (I): Characterization of flow boiling heat transfer. *International Journal of Heat and Mass Transfer.*, 2014,68: 703–715.
60. Carlo Bartoli, Federica Baffigi. Effects of ultrasonic waves on the heat transfer enhancement in subcooled boiling. *Experimental Thermal and Fluid Science.*, 2011,35:423–432.
61. Farzad Houshmand, Daren Elcock, Michael Amitay, Yoav Peles. Bubble formation from a micropillar in a microchannel. *International Journal of Multiphase Flow.*, 2014,59:44–53.
62. Woorim Lee, Gihun So. Numerical simulation of boiling enhancement on a microstructured surface. *International Communications in Heat and Mass Transfer.*, 2011,38: 168–173.
63. Rui Zhuan, Wen Wang. Flow pattern of boiling in micro-channel by numerical simulation. *International Journal of Heat and Mass Transfer.*, 2012,55:1741–1753.
64. Mushtaq I. Hasan, Rageba A.A, Yaghoubib M, Homayon Homayoni. Influence of channel geometry on the performance of a counter flow microchannel heat exchanger. *International Journal of Thermal Sciences.*, 2009,48:1607–1618.
65. Issam Mudawar. Experimental Investigation and Theoretical Model for Subcooled Flow Boiling Pressure Drop in Microchannel Heat Sinks. *Journal of Electronic Packaging.*, 2009, Vol. 131/ 031008-1.
66. Magnini M, Pulvirent B, Thome J.R. Numerical investigation of hydrodynamics and heat transfer of elongated bubbles during flow boiling in a microchannel. *International Journal of Heat and Mass Transfer.*, 2013,59:451–471.
67. Navin Raja Kuppusamy, Saidur R, Ghazali N.N.N, Mohammed H.A. Numerical study of thermal enhancement in microchannel heat sink with secondary flow. *International Journal of Heat and Mass Transfer.*, 2014,78: 216–223.
68. Woorim Lee, Gihun So, Han Young Yoon. Numerical study of bubble growth and boiling heat transfer on a microfinned surface. *International Communications in Heat and Mass Transfer.*, 2012,39: 52–57.

69. Sarangi R.K, Bhattacharya A, Prasher R.S. Numerical modelling of boiling heat transfer in microchannels. *Applied Thermal Engineering.*, 2009, 29: 300–309.
70. Tannaz Harirchian, Suresh V Garimella. Flow regime-based modeling of heat transfer and pressure drop in microchannel flow boiling. *International Journal of Heat and Mass Transfer.*, 2012,55: 1246–1260.
71. Balasubramanian K, Lee P.S, Jin L.W, Chou S.K, Teo C.J, Gao S. Experimental investigations of flow boiling heat transfer and pressure drop in straight and expanding microchannels - A comparative study. *International Journal of Thermal Sciences.*,2011,50: 2413-2421.

\*\*\*\*\*